

TIDAL VOLCANISM ON ENCELADUS. T. A. Hurford¹, J. N. Spitale², A. R. Rhoden³, W. G. Henning¹, and M. M. Hedman⁴, ¹NASA Goddard Space Flight Center, Greenbelt, MD 20771, ²Planetary Science Institute, Tucson, AZ 85719, ³Johns Hopkins University Applied Physics Lab., Laurel, MD 20723, ⁴University of Idaho, Moscow, ID 83844.

Introduction: Enceladus is a small (radius 250 km) moon that orbits Saturn between the moons Mimas and Tethys with a period of 1.37 days. This proximity to Saturn means that tidal dissipation should have quickly circularized the orbit. However, a 2:1 mean motion resonance with the moon Dione, which orbits just beyond Tethys, excites the orbital eccentricity to the observed value of 0.0047, which in turn produces periodic tidal stress on the surface.

In 2005, Cassini detected the eruption of material from warm regions, which correlated with the large Tiger Stripe fractures near the south pole of Enceladus [1,2]. While no temporal variation had been reported, a 2007 analysis of tidal stress postulated that the eruptive activity might be linked to tidal tension across these fractures and predicted that activity should vary on the orbital timescale such that greatest activity should be observed near apocenter [3]. Indeed, in 2013, results from analysis of Cassini's Visual and Infrared Mapping Spectrometer (VIMS) data confirmed the orbital variability of the erupting material and qualitatively confirmed the predictions of variable activity from 2007 [4,5].

Eruption Modeling and Depth of Volatile Reservoirs: Building off the simple models linking tensile stress on the Tiger Stripes with eruption activity [3,6,7], models were developed to fit activity seen in Cassini's Imaging Sub System (ISS) [8]. These models used shear, a phase lag in tidal response, or a physical libration to fit the observations. The later two mechanisms were invoked in order to explain the delay in eruption activity since the Tiger Stripes start to experience tension quite quickly after pericenter passage whereas the peak eruption output is later in the orbit.

The simple model linking the fraction of the Tiger Stripes in tension with the eruptive activity was useful to predict variable activity and that pericenter would be the most quiescent period within the orbit. However, it may be too simplified to reproduce finer variations within the orbital activity. For example, when the fraction of fractures experiencing tension rises, the tensile stresses on the surface are small or only slightly tensile. Thus, just beneath the surface the fracture would still be in compression and not likely to vent material.

By adding overburden stress to the tidal model, the tensile stress acting on the fractures can be analyzed at various depths. The overburden stress is linear with depth and works to compress the fracture, delaying activity in the orbit until tensile stresses are larger.

This naturally causes a lag in the orbital time at which fractures experience net tensile stress, potentially delaying the time of eruptive activity.

An additional simplification in earlier models is the use of the total fraction of Tiger Stripes in tension. With this approach, information about when different portions of the system first open in tension is lost. This assumption implies that the source of volatiles is not depleted during the eruptive cycle, which may not be physically justified. For example, after pericenter there is a rapid increase in the fraction of the system in tension. This fraction then remains constant for most of the orbit, predicting a broad period of more or less equal activity. However, the VIMS data seems steeply peaked around apocenter. During the period in which a steady fraction of Tiger Stripes is in tension, a small portion of the system is just starting to experience tension while others are switching to compression. The total fraction in tension is conserved, but the eruptive output may change as the tension on the fractures changes. If the quantity of volatiles in the reservoir is finite, then eruptive activity might be greatest just when a fracture first experiences tension and fall off as the fracture remains in tension. Therefore, our models focus on when the fracture first fails, allowing volatile escape.

Preliminary Results: Our first models investigated the activity predicted by tensile failure of a fracture at various depths. We find that the fits to activity are best for a depth of 1050m but require an addition of a constant amount of activity that is modulated by the activity induced by tensile failure. Fig. 1 shows the VIMS data we used for our modeling. The black solid curve is the result of tensile failure at 1050m depth. We have not yet added a phase lag, but it is possible that a lag may produce a better fit, and likely not be as large as those found by previous studies.

We did not limit our model to just tensile failure. At greater depths, fractures are not active in tension, but may fail in shear. We also model the Coulomb failure at greater depths. Fig. 1 shows one of our better fits at a shear failure depth of 2450m (dashed line).

Conclusions: Adding the depth of a volatile reservoir to models of tidal activity can naturally delay the timing of fracture failure, as seen in VIMS and ISS eruption activity on Enceladus. If tensile failure is directly linked to tidal activity then a phase lag may still be required. At the greatest depths of tensile failure, peaks in the timing of failure are still before apo-

center passage and not quite consistent with observations. Coulomb failure at greater depths might best match activity and does not require any additional phase lags or physical librations.

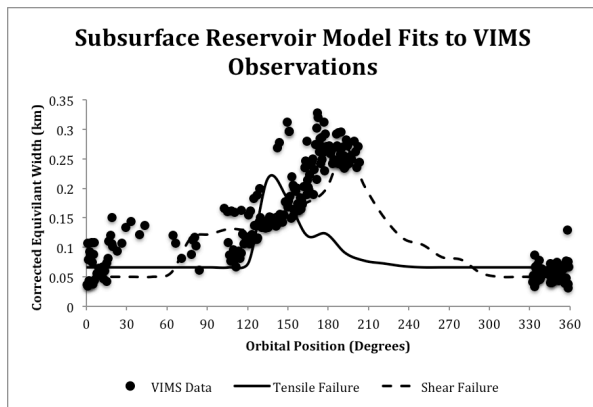


Fig. 1. Model fits to VIMS observations for two cases: 1) A constant output model plus activity based on tensile failure of the fracture system at a depth of 1050m and 2) A constant output model plus activity based on Coulomb failure of the fracture system at 2450m.

Tensile failure of the fracture system can only tap “shallow” sources (Fig. 2a). For model parameters used here, the maximum depth at which tensile failure can tap a volatile reservoir is about 1100m. This may prove problematic for the production and release of salt enriched ice grains. If the ice shell is 30-40 km thick [9], then the water table is approximately 3-4km below the surface and if salty ice grains are formed at a chamber of exposed sea water [10], then fractures must be able to fail in tension at this depth to allow the release of these types of grains through tensile failure. In order for tension to reach these depths, the h Love number would have to be larger (1 to 1.3). Since h is not known its possible but k would be larger and tidal heating would be greater than currently assumed.

Coulomb failure can reach to depths of the water table (Fig. 2b). In general, Coulomb failure acts to depths three times greater than tension. These failures can also facilitate release of volatiles closer to apocenter, without invoking any other mechanism (i.e. lags in response or physical libration). The ability to tap a liquid source at great depth may also account for variations in fracture temperatures seen on the surface. For example, the warmer branch of Baghdad sulcus can be active to significantly deeper depths.

Finally, there might be evidence of two active sources in the VIMS data. Post pericenter, there might be a smaller peak of activity before the main peak at apocenter. And the plume is made of arguably two components (salt-rich grains and salt-poor vapor). It may be that shallow sources of salt-poor vapor formed

within the fractures, and erupt early in the orbit, while salt-rich grains erupt later as deeper sources are tapped. This difference in eruptive material might be detectable within Cassini data.

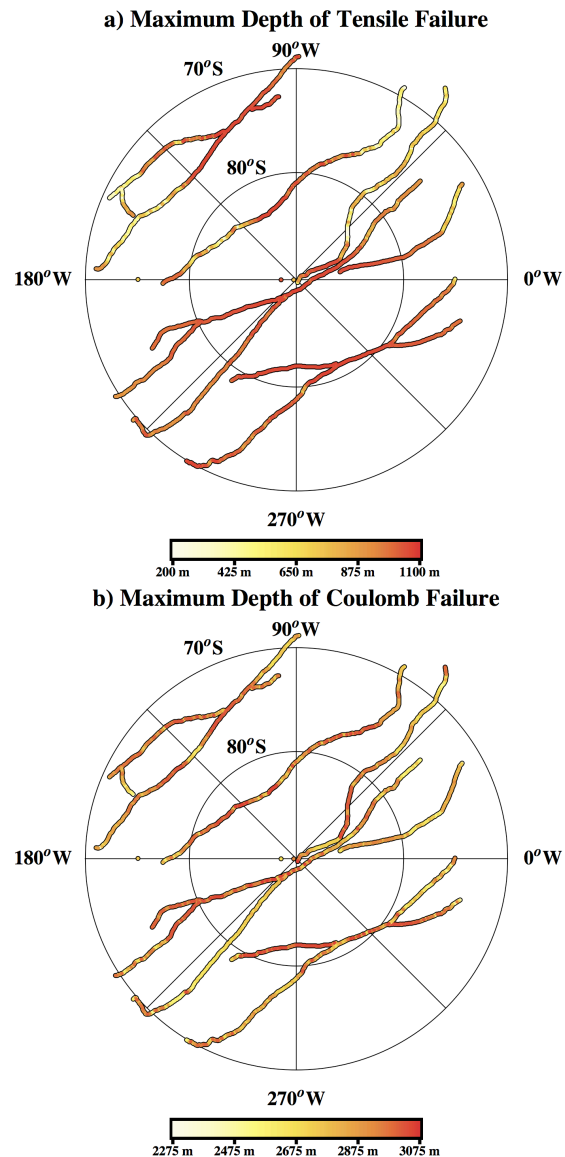


Fig. 2. a) The maximum depth at which tensile failure can occur and b) the maximum depth at which Coulomb failure is possible.

References: [1] Porco C.C. et al. (2006) *Science* 311, 1394-1401. [2] Spencer J.R. et al. (2006) *Science* 311, 1401-1405. [3] Hurford T.A. et al. (2007) *Nature* 447, 292-294. [4] Hedman M.M. et al. (2013) *Nature* 500, 182-184. [5] Spencer J.R. (2013) *Nature* 500, 155-156. [6] Hurford T.A. et al. (2009) *Icarus* 203, 541-552. [7] Hurford T.A. et al. (2012) *Icarus* 220, 896-903. [8] Nimmo F. et al. (2014) *Astro. J.* 148, 46. [9] Iess L. et al. (2014) *Science* 344, 78-80. [10] Postberg F. et al. (2011) *Nature* 474, 620-622.